

# Stability, Oxygen Nonstoichiometry, and Transformations of the $\text{Bi}_2\text{Sr}_2\text{CoO}_{6+\delta}$ Ceramic<sup>1</sup>

M. V. Zinkevich,<sup>2</sup> S. A. Prodan, Yu. G. Zonov, and V. V. Vashook

*Institute of General and Inorganic Chemistry, Belarussian Academy of Sciences, Surganova Str. 9, 220072, Minsk, Belarus*

Received February 27, 1996; in revised form December 4, 1996; accepted February 11, 1997

Thermogravimetry at 20–900°C and  $10^{-3}$ –1 atm of oxygen partial pressure ( $p\text{O}_2$ ) has been used to establish a region of stability and oxygen nonstoichiometry of the compound  $\text{Bi}_2\text{Sr}_2\text{CoO}_{6+\delta}$ . This phase was found to be unstable below 850°C at high oxygen partial pressures (air, oxygen), whereas at low oxygen concentrations in the gas phase ( $p\text{O}_2=1.5 \times 10^{-3}$ – $2 \times 10^{-2}$  atm) it exhibits stability in the entire temperature region under investigation. Within, the region of stability, the oxygen content in  $\text{Bi}_2\text{Sr}_2\text{CoO}_{6+\delta}$  ( $6+\delta$ ) has been determined under equilibrium conditions as a function of temperature and oxygen partial pressure and the corresponding defect model has been proposed. The annealing of  $\text{Bi}_2\text{Sr}_2\text{CoO}_{6+\delta}$  outside the region of stability is found to result in the formation of  $\text{Bi}_2\text{Sr}_3\text{Co}_2\text{O}_9$  and the binary compounds of the  $\text{Bi}_2\text{O}_3$ – $\text{SrO}$  system. The kinetics of this transformation has been studied at 700–850°C in a pure oxygen atmosphere and a possible interpretation has been given. © 1998 Academic Press

## 1. INTRODUCTION

Composite oxides of metals with mixed valences have received a great amount of attention from scientists dealing with solid state chemistry, since these oxides have a number of remarkable physicochemical properties which can easily be adjusted by changing the cationic composition and oxygen nonstoichiometry. Highly conductive rare-earth cobaltates doped with alkaline-earth cations are known to be promising materials for solid electrolyte devices (1). Recently, new compounds with somewhat high electronic conductivity containing cobalt, alkaline-earth metal, and bismuth have been discovered. These compounds have formulas such as  $\text{Bi}_2M_{n+1}\text{Co}_n\text{O}_y$  (where  $M = \text{Ca}, \text{Sr}, \text{Ba}$ ,  $n = 1, 2$ ) and they were first described in 1989 (2, 3) as the structural analogues of superconductive cuprates. However, the properties of these compounds are not yet well studied.

<sup>1</sup>This work was supported by the National Science Foundation of Belarus.

<sup>2</sup>To whom correspondence should be addressed. E-mail: admin@igic.basnet.minsk.by.

It has been shown that single-phase  $\text{Bi}_2\text{Sr}_2\text{CoO}_{6+\delta}$  can be obtained in air in the temperature region  $870 \pm 30^\circ\text{C}$ , whereas either lowering of the synthesis temperature in air or increasing oxygen partial pressure ( $p\text{O}_2$ ) near 800°C results in the formation of a multiphase system containing the  $\text{Bi}_2\text{Sr}_3\text{Co}_2\text{O}_9$  phase (2). It has also been found (2) that the heating of  $\text{Bi}_2\text{Sr}_2\text{CoO}_{6+\delta}$  powder in Ar to 500°C results in a 0.15% weight loss and about a 0.4% weight loss when the powder is heated to 800°C. The present paper is devoted to a more detailed investigation of stability, oxygen nonstoichiometry, and transformations of  $\text{Bi}_2\text{Sr}_2\text{CoO}_{6+\delta}$ .

## 2. EXPERIMENTAL

To prepare the polycrystalline  $\text{Bi}_2\text{Sr}_2\text{CoO}_{6+\delta}$  powder, chemically pure  $\text{Bi}_2\text{O}_3$ ,  $\text{Sr}(\text{NO}_3)_2$ , and  $\text{Co}(\text{NO}_3)_2 \cdot 6\text{H}_2\text{O}$  were used. The starting chemicals were mixed in the molar ratio  $\text{Bi}:\text{Sr}:\text{Co} = 2:2:1$  with an agate mortar and pestle under ethanol and dried at 80°C. The homogeneous product was placed in an alumina crucible and calcined in air at 300°C (2 h), 400°C (1 h), 600°C (3 h), and 800°C (4 h). After this procedure the powder was ground and fired again at 800°C (11 h). To obtain a single-phase material (4), the product obtained was pressed into pellets and refired in air at 930°C for 48 h.

The cationic composition of a sample was checked by chemical analysis with inaccuracy up to 0.5% of weight, according to (5, 6), after the dissolution of the powder in nitric acid. To determine the strontium and cobalt contents, the bismuth was previously separated in the form of  $\text{BiOCl}$ . To determine the primary oxygen content in  $\text{Bi}_2\text{Sr}_2\text{CoO}_{6+\delta}$ , the sample was placed in a quartz tube and annealed at 600°C for 1 h in a flow of dry pure hydrogen, and the weight loss was calculated. According to XRD data,  $\text{Bi}_2\text{Sr}_2\text{CoO}_{6+\delta}$  completely decomposes into Bi, Co, and SrO under these conditions. This experiment has been carefully arranged to exclude the loss of bismuth (e.g., bismuth vapors were precipitated as a mirror in the cold zone of the tube).

The investigation of oxygen nonstoichiometry was performed by thermogravimetry using a thermobalance, a

temperature controller, and a gas preparation system, allowing the detection of changes in weight down to  $3 \times 10^{-5}$  g (7). The sample, which had a weight of about 500 mg was studied under continuous heating and cooling ( $5^\circ\text{C}/\text{min}$ ), as well as under stepwise annealing to confirm the thermodynamic regime in the gas flow with the defined oxygen partial pressure. The same technique was used to study stability and transformations of  $\text{Bi}_2\text{Sr}_2\text{CoO}_{6+\delta}$  under isothermal conditions, and we observed the change of weight versus time. The ceramic samples for investigations were prepared by cold pressing powder ( $P = 5$  kbar) into tablets of 8-mm diameter and 1-mm thickness followed by sintering in air at  $900^\circ\text{C}$  for 5 h. An X-ray diffraction study of the ceramics and powders was carried out using a DRON-3 diffractometer ( $\text{CuK}\alpha$  radiation,  $U = 30$  kV,  $I = 10$  mA,  $2\Theta = 3^\circ\text{--}80^\circ$ ) before and after each experiment.

### 3. RESULTS AND DISCUSSION

#### 3.1. Phase Stability

To investigate the stability of  $\text{Bi}_2\text{Sr}_2\text{CoO}_{6+\delta}$  the sample weight was observed as a function of time at constant temperatures under ambient conditions with oxygen partial pressures  $p\text{O}_2$  of  $1.5 \times 10^{-3}$ , 0.02, 0.21, and 1.0 atm. The annealing temperatures were chosen in the interval  $200\text{--}900^\circ\text{C}$  with a step  $50^\circ\text{C}$ . At low oxygen partial pressures ( $1.5 \times 10^{-3}$  and 0.02 atm), after a small time for equilibration, the weight of a sample did not change within tens of hours. The same behavior was found at high  $p\text{O}_2$  (0.21 and 1.0 atm) except that at temperatures ranging from  $650$  to  $850^\circ\text{C}$ , we observed a continuous increase in weight. The XRD patterns of samples annealed under such conditions show that the system becomes multiphase.

Figure 1 shows the XRD patterns of the samples after they were annealed for 100 h at  $850^\circ\text{C}$  (a) and for 20 h at  $750^\circ\text{C}$  (b) in pure oxygen ( $p\text{O}_2 = 1$  atm). It is evident that along with the native  $\text{Bi}_2\text{Sr}_2\text{CoO}_{6+\delta}$  phase (2), significant amounts of  $\text{Bi}_2\text{Sr}_3\text{Co}_2\text{O}_9$  (3) and  $\text{Sr}_{0.9}\text{Bi}_{1.1}\text{O}_{2.75}$  (8) (Fig. 1a) or  $\text{Sr}_2\text{Bi}_2\text{O}_5$  (8) (Fig. 1b) are present. It should be noted that the same diffraction patterns as those shown in Fig. 1b have been obtained for the samples annealed at  $650\text{--}800^\circ\text{C}$ .

Because the oxidation degrees of cations in  $\text{Bi}_2\text{Sr}_3\text{Co}_2\text{O}_9$  are greater than those in  $\text{Bi}_2\text{Sr}_2\text{CoO}_6$ , one might suppose that the oxygen content in  $\text{Bi}_2\text{Sr}_2\text{CoO}_{6+\delta}$  cannot be higher than a certain value. When excessive oxygen is introduced into the lattice, which is achievable at  $850^\circ\text{C}$  and lower temperatures in ambient air or oxygen, this phase becomes unstable, as pointed out in the literature (2). Below  $650^\circ\text{C}$  the  $\text{Bi}_2\text{Sr}_2\text{CoO}_{6+\delta}$  phase seems to be metastable, although we could not observe the increase in weight during annealing because the transformation appeared to proceed very slowly.

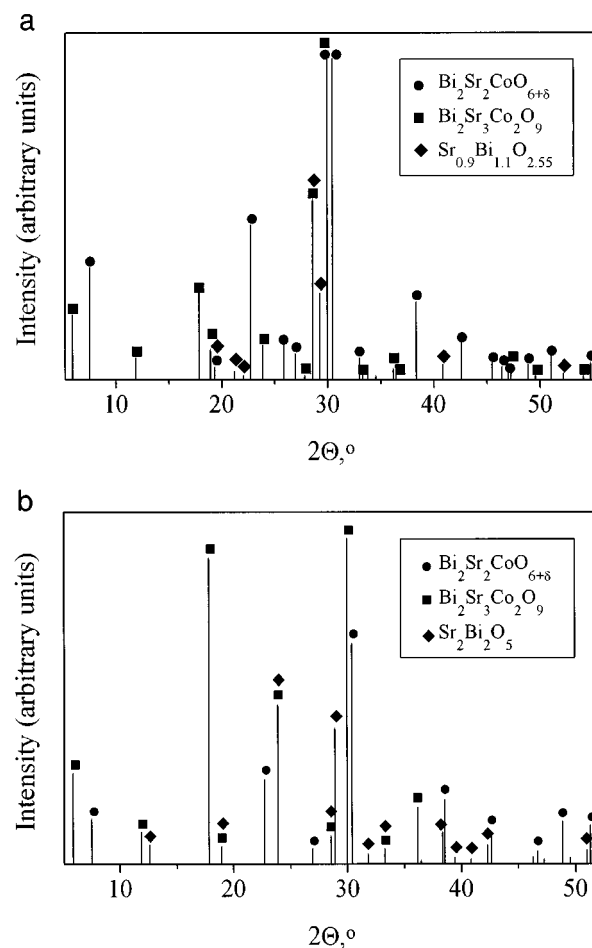


**FIG. 1.** X-ray diffraction patterns of the  $\text{Bi}_2\text{Sr}_2\text{CoO}_{6+\delta}$  sample after it was annealed for (a) 100 h at  $850^\circ\text{C}$  for (b) and 20 h at  $750^\circ\text{C}$  in pure oxygen ( $p\text{O}_2 = 1$  atm).

To elucidate whether the transformation of  $\text{Bi}_2\text{Sr}_2\text{CoO}_{6+\delta}$  is reversible, the following experiment has been performed: after being annealed for 100 h at  $850^\circ\text{C}$  in oxygen and cooled down to room temperature, the sample was heated again in air to  $900^\circ\text{C}$  and annealed for 2 h. X-ray powder diffraction analysis of the sample after it cooled to room temperature showed that the material completely turned back into  $\text{Bi}_2\text{Sr}_2\text{CoO}_{6+\delta}$ .

#### 3.2. Oxygen Nonstoichiometry

The variation of the oxygen content ( $6 + \delta$ ) in  $\text{Bi}_2\text{Sr}_2\text{CoO}_{6+\delta}$  ceramic with temperature in atmospheres of pure oxygen (1), air (2), a mixture of helium + oxygen (3), and pure helium (4) is shown in Fig. 2. Below  $400^\circ\text{C}$  no changes in sample weight are observed. Increasing or decreasing the temperature in the region  $400\text{--}900^\circ\text{C}$  and isothermal annealing resulted in the same value of oxygen content for each temperature point, indicating the achievement of

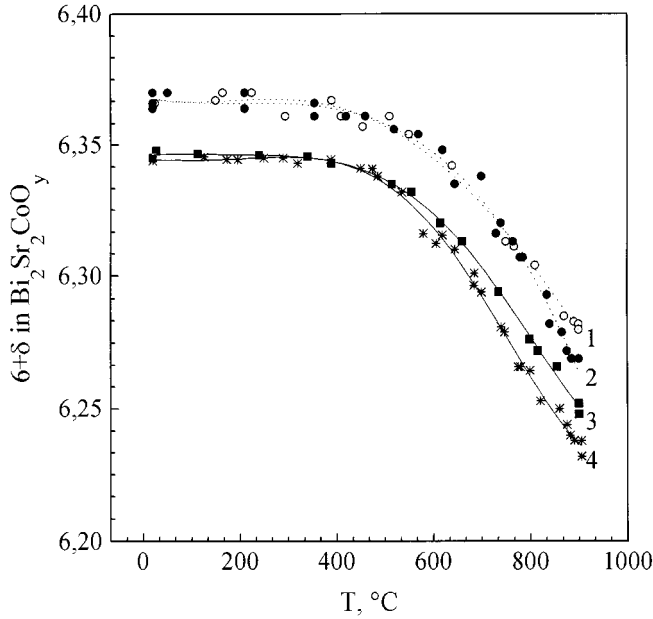


FIG. 2. Oxygen content in Bi<sub>2</sub>Sr<sub>2</sub>CoO<sub>6+δ</sub> as a function of temperature at oxygen partial pressures: (1) 1.0, (2) 0.21, (3) 0.02 and (4)  $1.5 \times 10^{-3}$  atm.

equilibrium in this type of experiment. The dashed line in Fig. 2 corresponds to the trace of oxygen content outside the region of stability when the sample cooled from 900°C with the rate 5°C/min. These conditions probably allow the determination of  $\delta$  values for metastable Bi<sub>2</sub>Sr<sub>2</sub>CoO<sub>6+δ</sub> until the transformation rate becomes appreciable. In any case, we could not observe any changes in the X-ray diffraction patterns after such treatment.

With the oxygen nonstoichiometry known, it is possible to reach a conclusion about the oxidation degrees of metal cations in Bi<sub>2</sub>Sr<sub>2</sub>CoO<sub>6+δ</sub>. According to (2), the oxidation degree for bismuth in this compound can be only +3. Thus, whatever changes in the oxygen content occur, they should result in changes in the valence state of cobalt ions. Assuming this model, the oxygen content  $\delta = 0$  corresponds to all bivalent cobalt and  $\delta = 0.5$  to all trivalent cobalt. Hence, the chemical formula of Bi<sub>2</sub>Sr<sub>2</sub>CoO<sub>6+δ</sub> may be presented as Bi<sub>2</sub><sup>3+</sup>Sr<sub>2</sub><sup>2+</sup>Co<sub>1-2δ</sub><sup>2+</sup>Co<sub>2δ</sub><sup>3+</sup>O<sub>6+δ</sub><sup>2-</sup>, where  $\delta$  for our experimental conditions lies in the range 0.23–0.37.

Finally, we have made an attempt to deduce the defect structure of Bi<sub>2</sub>Sr<sub>2</sub>CoO<sub>6+δ</sub> from the nonstoichiometry data.

The first assumption, based on structural studies (2), was that the predominant defects in Bi<sub>2</sub>Sr<sub>2</sub>CoO<sub>6+δ</sub> are interstitial oxygen ions. The layered structure of this compound allows easy insertion of oxygen between the layers, when the average valence of cobalt remains between +2 and +3. In contrast to produce the oxygen vacancies, some layers should be partially destroyed, and the average valence of Co would be less than +2.

Applying the point defects model, developed by Kröger (9), one can obtain the equations



$$K_{\text{ox}} = \frac{[\text{O}_i'] \cdot p^2}{(p\text{O}_2)^{1/2}}, \quad [2]$$

where  $[\text{O}_i']$  is the concentration of oxygen interstitials,  $p$  the concentration of electronic holes, and  $K_{\text{ox}}$  the equilibrium constant for oxygen insertion process.

The second assumption was that we are in the “high  $p\text{O}_2$  region,” where the electroneutrality condition

$$2[\text{O}_i'] + n = 2[V_o''] + p \quad [3]$$

may be simplified to

$$p = 2[\text{O}_i'] \quad [4]$$

Then, combining Eqs. [4] and [2], one can obtain

$$K_{\text{ox}} = \frac{4[\text{O}_i']^3}{(p\text{O}_2)^{1/2}} \quad [5]$$

Using the expression for the equilibrium constant  $\Delta G = -RT \ln K$ , Eq. [5] may be rewritten as

$$-\frac{\Delta G_{\text{ox}}}{RT} = \ln 4 + 3 \ln [\text{O}_i'] - \frac{1}{2} \ln (p\text{O}_2), \quad [6]$$

where  $\Delta G_{\text{ox}}$  is the Gibbs energy of oxygen interstitial formation. Thus, the oxygen partial pressure, providing fixed oxygen interstitial concentration, may be expressed as a function of temperature:

$$\ln (p\text{O}_2) = 2 \ln 4 + 6 \ln [\text{O}_i'] + \frac{2\Delta G_{\text{ox}}}{RT} \quad [7]$$

By plotting  $\ln (p\text{O}_2)$  versus reciprocal temperature, the values of  $\Delta G_{\text{ox}}$  can be easily obtained.

Figure 3 represents such plots for different nonstoichiometry values ( $\delta$ ) in Bi<sub>2</sub>Sr<sub>2</sub>CoO<sub>6+δ</sub>. It is evident that a straight-line dependence of  $\ln (p\text{O}_2)$  versus  $1/T$  with almost the same slope is preserved for  $\delta$  values in the range 0.270–0.304, whereas at higher oxygen content the simple point defect model appears to be not applicable. Nevertheless, we have made attempts to calculate the corresponding Gibbs energies for this region also, which all are summarized in Table 1.

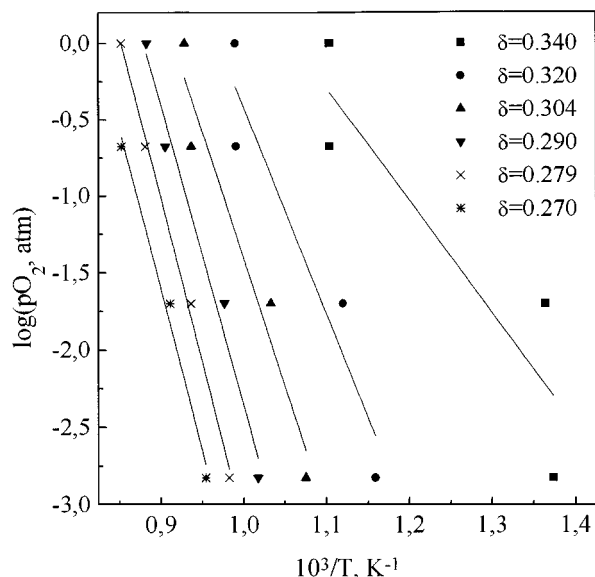
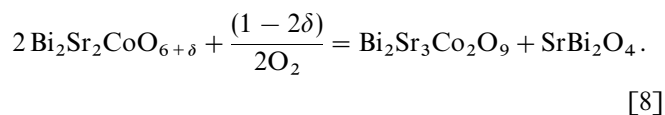


FIG. 3. Equilibrium oxygen partial pressures providing fixed oxygen nonstoichiometry in  $\text{Bi}_2\text{Sr}_2\text{CoO}_{6+\delta}$  as a function of temperature.

### 3.3. Transformations

**3.3.1. Thermodynamics.** As mentioned above, the annealing of  $\text{Bi}_2\text{Sr}_2\text{CoO}_{6+\delta}$  outside its region of stability leads to the formation of  $\text{Bi}_2\text{Sr}_3\text{Co}_2\text{O}_9$  and one of the binary oxides,  $\text{Sr}_{0.9}\text{Bi}_{1.1}\text{O}_{2.55}$  or  $\text{Sr}_2\text{Bi}_2\text{O}_5$ , depending on the temperature. It should be noted, however, that to satisfy the mass balance, the reaction must proceed according to the equation



Nevertheless, the stoichiometry of products such as  $\text{Sr}_{0.9}\text{Bi}_{1.1}\text{O}_{2.55}$  or  $\text{Sr}_2\text{Bi}_2\text{O}_5$  clearly indicates the lack of about 1 mol of bismuth. The loss of the latter due to evapor-

TABLE 1  
The Gibbs Energies for Oxygen Interstitial Formation  
in  $\text{Bi}_2\text{Sr}_2\text{CoO}_{6+\delta}$

$\delta$	$\Delta G_{\text{ox}}$ (kJ/mol)
0.270	$-87 \pm 10$
0.279	$-88 \pm 4$
0.290	$-82 \pm 8$
0.304	$-69 \pm 12$
0.320	$-56 \pm 12$
0.340	$-30 \pm 10$

ation can be ruled out, because the annealing of a sample at  $900^\circ\text{C}$  for 60 h did not result in an appreciable change in weight. Therefore, it may be supposed that either an absent bismuth compound is amorphous or its peaks on the diffraction patterns are overlapped by others.

Since the  $\text{SrBi}_2\text{O}_4$  compound has a tendency to decompose (10) into two solid solutions, tetragonal  $\gamma$  ( $\text{Sr}_{0.9}\text{Bi}_{1.1}\text{O}_{2.55}$ ) and rhombohedral  $\beta$  ( $\text{Bi}_{1-x}\text{Sr}_x\text{O}_{1.5-x/2}$ ), the composition of which may be in the range  $0.10 \leq x \leq 0.27$ , the “hidden” bismuth seems to be introduced in that rhombohedral solid solution. However, the main peaks corresponding to the latter in the X-ray diffraction pattern (11) appear to be overlapped by extremely intense [001] reflections coming from  $\text{Bi}_2\text{Sr}_2\text{CoO}_{6+\delta}$  and  $\text{Bi}_2\text{Sr}_3\text{Co}_2\text{O}_9$  (see Fig. 1). At the same time, we are not in a position to confirm unambiguously the presence of this phase because its exact composition is unknown.

The differences in the products after they are annealed at  $850^\circ\text{C}$  and lower temperatures may be explained by referring to the state diagram of the  $\text{Bi}_2\text{O}_3$ – $\text{SrO}$  system (8). It is quite evident that the  $\gamma$  solid solution is unstable at  $800^\circ\text{C}$  and lower temperatures, so that its formation is suppressed, giving  $\text{Sr}_2\text{Bi}_2\text{O}_5$  instead.

Furthermore, the layered modulated structure of  $\text{Bi}_2\text{Sr}_2\text{CoO}_{6+\delta}$  (2) appears to promote the decomposition of  $\text{SrBi}_2\text{O}_4$  even at temperatures lower than  $800^\circ\text{C}$  where this phase should be stable, according to the state diagram (8). Indeed, considering the plot of projection of the  $\text{Bi}_2\text{Sr}_2\text{CoO}_{6+\delta}$  structure, taken from (2) (Fig. 4), one can see alternating Bi-rich and Bi-deficient zones. They produce local inhomogeneity regions with different bismuth content per arbitrary volume. Therefore, it is probable that Bi-rich zones become the nuclei of phase  $\beta$ , which contains more bismuth than  $\text{SrBi}_2\text{O}_4$ , and Bi-deficient zones result

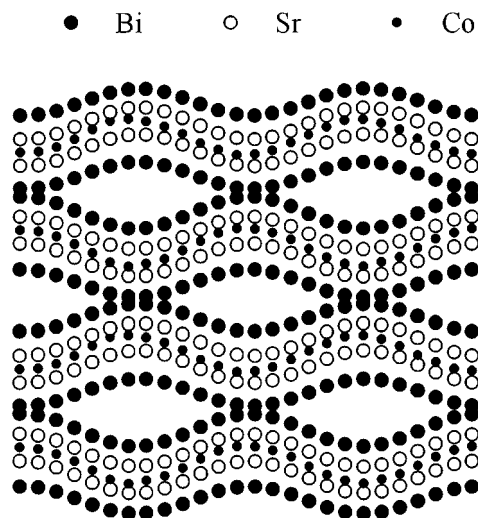


FIG. 4. A plot of projection of  $\text{Bi}_2\text{Sr}_2\text{CoO}_{6+\delta}$  structure, taken from (2).

information of the nuclei of Sr<sub>2</sub>Bi<sub>2</sub>O<sub>5</sub>. Such inhomogeneity on the atomic level seems to be a reason for the absence of SrBi<sub>2</sub>O<sub>4</sub> in the XRD patterns.

**3.3.2. Kinetics: Model.** As follows from previous considerations, the transformation of Bi<sub>2</sub>Sr<sub>2</sub>CoO<sub>6+δ</sub> is due to its interaction with oxygen. Thus, the overall reaction may be subdivided into several steps:

1. adsorption of molecular oxygen on the surface;
2. ionization of O<sub>2</sub> molecules and dissolution of oxygen in the lattice;
3. diffusion of interstitial oxygen to the product–reagent interface;
4. chemical reaction.

The interaction of Bi<sub>2</sub>Sr<sub>2</sub>CoO<sub>6+δ</sub> with molecular oxygen seems to be negligible because it can occur only in the initial stage when the surface is not yet covered by products.

Assuming the quasistationarity condition, the overall kinetics will be determined by the stage having the lowest rate (e.g., limiting step). Therefore, the total kinetic equation should be similar to the kinetic equation describing one of the above-mentioned elementary steps, depending on what step is limiting in the corresponding reaction period. Such “partial” kinetic equations can be obtained from the theory of heterogeneous reactions (12, 13) (Table 2), where  $k_a$ ,  $k_i$ ,  $k_D$ ,  $k_N$ , and  $k_1$  mean the formal rate constants for adsorption, ionization, diffusion, nucleation, and first-order reaction, respectively,  $pO_2$  is the oxygen partial pressure and  $\alpha$  is the conversion rate.

**3.3.3. Kinetics: Experimental results.** Kinetic curves obtained by isothermal TGA measurements in pure oxygen ( $pO_2 = 1$  atm) are shown in Fig. 5. Because all the reaction products were assumed to be stoichiometric, but Bi<sub>2</sub>Sr<sub>2</sub>CoO<sub>6+δ</sub> exhibited an appreciable oxygen nonstoichiometry with temperature, the following expression has been used to calculate the conversion rate ( $\alpha$ ),

$$\alpha = \frac{(\Delta m/m_0)_t}{(\Delta m/m_0)_\infty} \quad [9]$$

$$(\Delta m/m_0)_\infty = \frac{16(1 - 2\delta)}{1496.26 + 32\delta}, \quad [10]$$

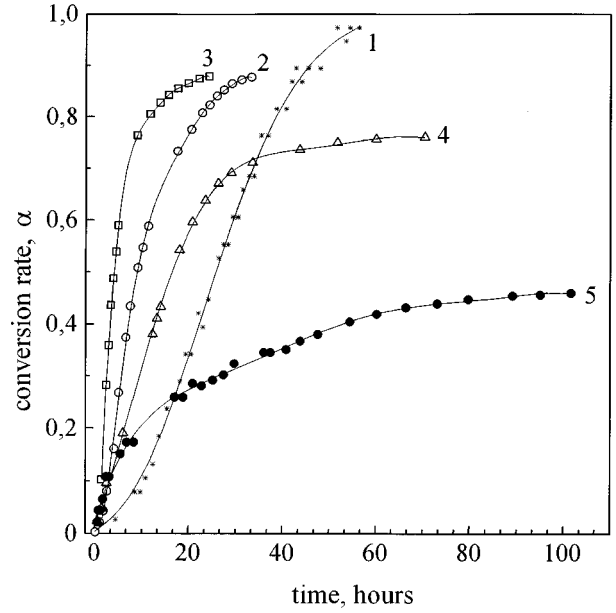


FIG. 5. Isothermal kinetics of transformation of Bi<sub>2</sub>Sr<sub>2</sub>CoO<sub>6+δ</sub> in pure oxygen ( $pO_2 = 1$  atm).

where  $(\Delta m/m_0)_t$  is the weight gain observed at time  $t$  and  $(\Delta m/m_0)_\infty$  is the theoretical weight gain corresponding to complete proceeding of reaction [8].

The results obtained (Fig. 5) clearly indicate that the depth of the transformation, as well as the kinetics, is dramatically influenced by temperature. Indeed, a conversion rate near 100% is achieved only for temperatures of 700–750°C (curves 1–3), whereas at higher temperatures the transformation proceeds significantly more slowly, limiting the conversion rate to 0.73 and 0.44 for 800 and 850°C, respectively (curves 4, 5 in Fig. 5). The maximum transformation rate has been observed at 750°C.

It should also be noted that only two curves (1, 2) have a well-defined sigmoidal shape, which is frequently attributed to topochemical reactions (12), whereas for the remaining curves (3–5) the so-called “induction period” could not be detected.

TABLE 2  
Possible Limiting Steps and Corresponding Kinetic Equations for Gas–Solid Heterogeneous Reactions

	Limiting step	Kinetic equation	Localization
Adsorption	$O_2(g) \rightleftharpoons O_2(ads.)$	$\alpha = k_a \cdot pO_2 \cdot t$	Gas–solid interface
Ionization	$\frac{1}{2} O_2(ads.) \rightleftharpoons O_i'' + 2h'$	$\alpha = k_a \cdot k_i \cdot pO_2 \cdot t$	Adsorption layer
Diffusion	$O_i''(surface) \rightarrow O_i''(bulk)$	$\alpha = k_D \cdot t^{1/n}, n > 1$	Ceramic bulk
Chemical reaction (nucleation and growth of nuclei)	$2Bi_2Sr_2CoO_{6+\delta} + O_i'' + 2h' =$	$\alpha = k_N \cdot t^n, n = 2, 3, 4$	
Chemical reaction (the decay period)	$Bi_2Sr_3Co_2O_9 + SrBi_2O_4$	$\alpha = 1 - \exp(-k_1 \cdot t)$	Product–reagent interface

3.3.4. *Kinetics: Comparison of theory with experiment.* As stated above, theory predicts four possible limiting steps for the transformation of  $\text{Bi}_2\text{Sr}_2\text{CoO}_{6+\delta}$  (see Table 2). Because each step is characterized by a specific kinetic equation, each experimental curve (or part of it) should fit one of the “partial” equations indicated above for the given region of conversion rate, provided that the quasistationarity condition is valid (e.g., one and only one stage of the complex process is limiting).

Assuming adsorption or ionization as a limiting step, one would expect to obtain a straight line in  $(\alpha-t)$  coordinates. However, Fig. 5 shows that this is not the case. Therefore, it can be concluded that neither adsorption nor ionization can limit the overall kinetics.

Furthermore, one might suppose that kinetics is controlled by the chemical reaction. Then, at a low conversion rate the entire process should be limited by nucleation and growth of nuclei, whereas in the last stages an exponential decay law can be expected (see Table 2). The most common equation, relating the conversion rate ( $\alpha$ ) to the reaction time ( $t$ ), when the limiting step is nucleation followed by growth of nuclei is given by Delmon (12),

$$\alpha = k_N \cdot (t - t_i)^{p+q+1}, \quad [11]$$

where  $k_N$  is the nucleation constant,  $t_i$  the induction period, and  $p$  and  $q$  are the integer numbers, depending on the type of nucleation and the growth of nuclei. Following this approach, a plot of  $\log(\alpha)$  versus  $\log(t)$  should fit to a straight line. The slope of this line should give the  $p + q + 1$  value and the intercept with the vertical axis determines  $k_N$ .

Our attempts to perform this approximation are shown in Fig. 6. It is easy to see that the proposed model gives satisfactory results only for curves obtained at 700, 725, and probably 750°C. For the last case, unfortunately, no data have been obtained for the small times due to the greatest acceleration. Nevertheless, the shape of this curve indicates that the behavior of  $\text{Bi}_2\text{Sr}_2\text{CoO}_{6+\delta}$  at 750°C appears to be similar to that at lower temperatures. These three curves are characterized by almost identical slopes, giving the value of the exponent in Eq. [11]  $\approx 2$ . Moreover, the region of conversion rates where the considered model can be applied is almost the same for all three temperatures, 700, 725, and 750°C, reaching the value of  $\alpha \approx 0.44$  (Fig. 6).

According to (12), the value found for the exponent may be attributed to

- (a) nucleation with constant rate ( $q = 0$ ) and one-dimensional growth ( $p = 1$ );
- (b) instantaneous nucleation ( $q = -1$ ) and two-dimensional growth ( $p = 2$ ).

With reference to the layered structure of  $\text{Bi}_2\text{Sr}_2\text{CoO}_{6+\delta}$  it may be suggested that two-dimensional growth of nuclei between the layers seems to be more favorable, and therefore case (b) is more probable.

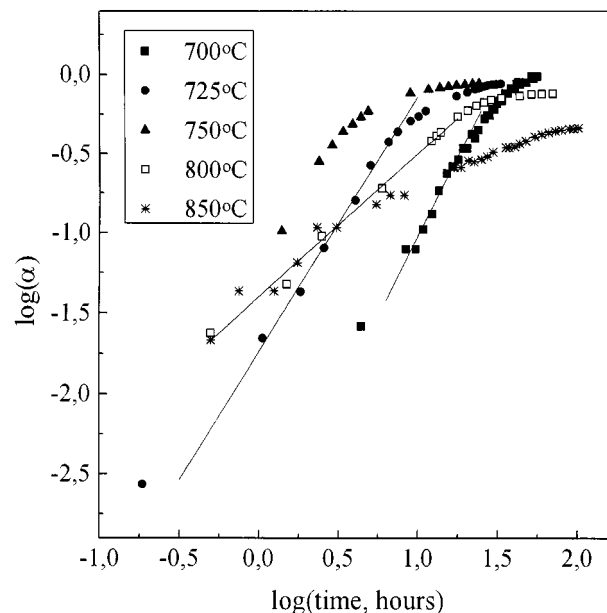


FIG. 6. Fitting of the experimental kinetic curves of transformation of  $\text{Bi}_2\text{Sr}_2\text{CoO}_{6+\delta}$  to the equation  $\log(\alpha) = \text{const} + n \cdot \log(t)$ , assuming that the limiting step is the chemical reaction.

The values of  $k_N$  corresponding to the intercept of fitting lines with the vertical axis (Fig. 6) tend to increase with temperature. This is an additional confirmation that the limiting step is the chemical reaction.

It should be noted that some initial points lie slightly above the corresponding fitting lines, indicating the induction period required to form the nuclei of products on the gas–solid interface.

Attempts to fit the curves obtained at 800 and 850°C to Eq. [11] gave an unusual value of less than 1 for the exponents. Theory cannot explain such dependence, assuming the chemical reaction as a limiting step. Furthermore, the fitting curves completely coincide for these temperatures. Such results provide evidence that at temperatures as high as 800°C the chemical reaction is not the limiting step. A fitting of the equation, describing the “decay period” (see Table 2), gave positive results only for one curve, recorded at 700°C. Thus it may be concluded that at this temperature the transformation of  $\text{Bi}_2\text{Sr}_2\text{CoO}_{6+\delta}$  is completely controlled by chemical reaction.

With regard to the remaining temperatures, it should be noted that diffusion limitation appears to play an important role, especially in the final period. However, a simple “parabolic” diffusion law (13) proved to be inconsistent for all the temperatures. A fitting of the final parts of curves for 725–850°C in Fig. 6 to straight lines resulted in exponent values ( $n$ ) from 0.15 to 0.42. No simple model known from the literature can explain such results. Thus, the quasistationary condition seems to be invalid and one limiting step cannot be isolated. One might suppose that the

chemical reaction and the diffusion contribute to limitation of the overall process.

#### 4. CONCLUSIONS

The stability and oxygen nonstoichiometry of the compound Bi<sub>2</sub>Sr<sub>2</sub>CoO<sub>6+δ</sub> have been studied. This phase is stable in reducing atmospheres up to 900°C and above 850°C in an oxidizing environment.

The point defect model, assuming interstitial oxygen, can be used to describe the nonstoichiometry of Bi<sub>2</sub>Sr<sub>2</sub>CoO<sub>6+δ</sub> in the range  $\delta = 0.27-0.30$ .

In air or oxygen, when the temperature is lower than 850°C, Bi<sub>2</sub>Sr<sub>2</sub>CoO<sub>6+δ</sub> transforms into Bi<sub>2</sub>Sr<sub>3</sub>Co<sub>2</sub>O<sub>9</sub> and the binary compounds of the Bi<sub>2</sub>O<sub>3</sub>-SrO system. The kinetics of this transformation in a pure oxygen atmosphere has been studied at different temperatures. The transformation was found to be fastest at 750°C. At lower temperatures (700-750°C) the overall process is controlled by chemical reaction, at least in the initial stage, which probably can be attributed to instantaneous nucleation and two-dimensional growth of nuclei. At higher temperatures (800-850°C) the limiting step cannot be isolated. The growing influence of diffusion deceleration appears to result in a small conversion rate in this temperature region, even for large times of exposure.

#### REFERENCES

1. E. Ivers-Tiffée, M. Schiessl, H. J. Oel, and W. Wersing, in "Proc. 14th Risoe Int. Symp. on Materials Science" (Poulsen, Bentzen, Jacobsen, Skou, and Ostergard, Eds.), p. 69. Risoe National Lab., Roskilde, Denmark.
2. J. M. Tarascon, P. F. Miceli, P. Barboux, D. M. Hwang, G. W. Hull, M. Giroud, L. H. Greene, *et al.*, *Phys. Rev. B* **39**, 11587 (1989).
3. J. M. Tarascon, R. Ramesh, P. Barboux, M. S. Hedge, G. W. Hull, L. H. Greene, M. Giroud, Y. LePage, W. R. McKinnon, J. V. Waszczak, and L. F. Schneemeyer, *Solid State Commun.* **71**, 663 (1989).
4. Y. Matsui, K. Kishio, Y. Tomioka, T. Hasegawa, and S. Ikeda, *Jpn. J. Appl. Phys.* **28**, L1991 (1989).
5. G. Charlot, in "Les methodes de la chimie analytique," pp. 733, 1015. (Masson), Paris, 1961.
6. G. Schwarzenbach and H. Flaschka, in "Die komplexometrische Titration" (Ferdinand Enke, Ed.), p. 243, Verlag, Stuttgart, 1965.
7. V. V. Vashook, S. A. Prodan, M. V. Zinkevich, and O. P. Olshevskaya, *Neorg. Mater.* **29**, 641 (1993).
8. R. S. Roth, C. J. Rawn, B. P. Burton, and F. Beech, *J. Res. Natl. Stand. Technol.* **95**, 291 (1990).
9. F. A. Kröger, "The Chemistry of Imperfect Crystals," North-Holland, Amsterdam, 1964.
10. P. Conflant, M. Drache, J. P. Wignacourt, and J. C. Boivin, *Mater. Res. Bull.* **26**, 1219 (1991).
11. A. Watanabe, *Solid State Ionics* **35**, 281 (1989).
12. B. Delmon, "Introduction a la cinetique heterogene." Editions Techip, Paris, 1969.
13. W. E. Garner, "The Chemistry of the Solid State." Butterworth Scientific, London, 1955.